LETTER

doi:10.1038/nature14320

Tetanus toxoid and CCL3 improve dendritic cell vaccines in mice and glioblastoma patients

Duane A. Mitchell[1,2,3]*, Kristen A. Batich[2,3]*, Michael D. Gunn[4,5], Min-Nung Huang[5], Luis Sanchez-Perez[2], Smita K. Nair[6], Kendra L. Congdon[2], Elizabeth A. Reap[2], Gary E. Archer[1,2], Annick Desjardins[1,2], Allan H. Friedman[1,2], Henry S. Friedman[1,2], James E. Herndon II[7], April Coan[7], Roger E. McLendon[1,3], David A. Reardon[1,2], James J. Vredenburgh[1,2], Darell D. Bigner[1,2,3] & John H. Sampson[1,2,3,5,8]

After stimulation, dendritic cells (DCs) mature and migrate to draining lymph nodes to induce immune responses[1]. As such, autologous DCs generated *ex vivo* have been pulsed with tumour antigens and injected back into patients as immunotherapy. While DC vaccines have shown limited promise in the treatment of patients with advanced cancers[2–4] including glioblastoma[5–7], the factors dictating DC vaccine efficacy remain poorly understood. Here we show that pre-conditioning the vaccine site with a potent recall antigen such as tetanus/diphtheria (Td) toxoid can significantly improve the lymph node homing and efficacy of tumour-antigen-specific DCs. To assess the effect of vaccine site pre-conditioning in humans, we randomized patients with glioblastoma to pre-conditioning with either mature DCs[8] or Td unilaterally before bilateral vaccination with DCs pulsed with *Cytomegalovirus* phosphoprotein 65 (pp65) RNA. We and other laboratories have shown that pp65 is expressed in more than 90% of glioblastoma specimens but not in surrounding normal brain[9–12], providing an unparalleled opportunity to subvert this viral protein as a tumour-specific target. Patients given Td had enhanced DC migration bilaterally and significantly improved survival. In mice, Td pre-conditioning also enhanced bilateral DC migration and suppressed tumour growth in a manner dependent on the chemokine CCL3. Our clinical studies and corroborating investigations in mice suggest that pre-conditioning with a potent recall antigen may represent a viable strategy to improve anti-tumour immunotherapy.

To evaluate the influence of vaccine site pre-conditioning on DC migration clinically, we conducted a randomized and blinded clinical trial in newly diagnosed glioblastoma (GBM) (Extended Data Fig. 1). A total of 13 patients consented to this trial but only 12 were randomized as 1 progressed before randomization (Extended Data Table 1). Patients were randomized to unilateral vaccine site pre-conditioning with unpulsed, autologous DCs[8] or Td, on the basis of our hypothesis that it would induce inflammation at the vaccine site[13]. The accumulation of injected DCs in vaccine site-draining lymph nodes (VDLNs) was significantly greater in patients given Td (Fig. 1a). Moreover, Td-treated patients also showed a significant increase in both progression-free survival (Fig. 1b) and overall survival (Fig. 1c) compared to DC-treated patients. From the time of diagnosis, patients in the DC cohort had median progression-free and overall survivals of 10.8 and 18.5 months, respectively. Thus, the median progression-free and overall survivals for the DC cohort were consistent with patients treated with the standard of care[14]. Three censored patients from the Td cohort did not progress and were alive at the time of survival analysis (>36.6 months). Overall, these prognostic factors varied across both treatment groups as expected in a small clinical trial. However, there was no discernible trend across prognostic factors that would suggest that these factors alone account for the observed differences in survival between cohorts. Using both a previously published recursive partition analysis[15] and the European Organization for Research and Treatment of Cancer (EORTC) nomogram[16] for predicting outcome of patients with GBM, Td-treated patients exceeded expected survival times by a far greater degree than did DC-treated patients in both cases by nearly the same amount (Extended Data Table 1). The vaccine responses in long-term survivors varied in durability, but pp65-specific

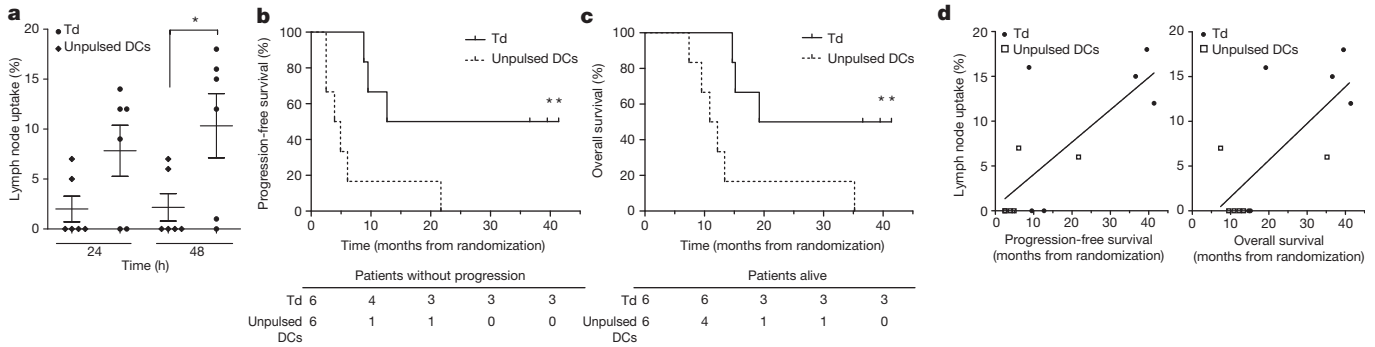

Figure 1 | Td pre-conditioning increases DC migration to VDLNs and is associated with improved clinical outcomes. **a**, DC migration in Td ($n = 6$) versus unpulsed DC ($n = 6$) patients (two sample t-test, $P = 0.049$). Mean ± s.e.m., n values represent biological replicates of patient bilateral inguinal lymph nodes (iLNs). **b**, **c**, Patient progression-free survival (**b**) and overall survival (**c**) (log-rank test, $P = 0.013$). **d**, Hazard ratios (HRs): DC migration efficiency from Td and DC cohorts showing the effect of a 1-unit increase in the percentage migration on progression-free (left) and overall (right) survival (Cox proportional hazards model, progression-free survival HR = 0.845 $P = 0.027$; overall survival HR = 0.820 $P = 0.023$). In **b** and **c**, $n = 3$ censored Td patients (no progressive disease at survival analysis).

[1]Preston Robert Tisch Brain Tumor Center, Duke University Medical Center, Durham, North Carolina 27710, USA. [2]Division of Neurosurgery, Department of Surgery, Duke University Medical Center, Durham, North Carolina 27710, USA. [3]Department of Pathology, Duke University Medical Center, Durham, North Carolina 27710, USA. [4]Division of Cardiology, Department of Medicine, Duke University Medical Center, Durham, North Carolina 27710, USA. [5]Department of Immunology, Duke University Medical Center, Durham, North Carolina 27710, USA. [6]Division of Surgical Sciences, Department of Surgery, Duke University Medical Center, Durham, North Carolina 27710, USA. [7]Department of Biostatistics and Bioinformatics, Duke University Medical Center, Durham, North Carolina 27710, USA. [8]Department of Radiation Oncology, Duke University Medical Center, Durham, North Carolina 27710, USA.
*These authors contributed equally to this work.

©2015 Macmillan Publishers Limited. All rights reserved

immune responses were detectable for several months in all long-term survivors. An increase in pp65-specific interferon-γ spot-forming units from baseline did correlate with overall survival, and the two long-term survivors for which samples were available had the highest increases in pp65-specific immune responses after vaccination. In addition, we observed a notable association between DC migration to the VDLNs and progression-free and overall survival (Fig. 1d) in patients with GBM receiving pp65 RNA-pulsed DC vaccines.

To validate these clinical results and understand the mechanistic underpinnings, we performed analogous studies in a mouse model. Vaccine sites of Td-immune mice were pre-conditioned with Td and then received a bilateral vaccine of ovalbumin (OVA) RNA-pulsed DCs. In parallel to our clinical findings, Td-immune mice receiving Td pre-conditioning had a threefold increase in DCs within the afferent inguinal lymph nodes (Fig. 2a). This effect was attributable to Td-specific recall responses as mice not primed with Td (Td-naive mice) did not display any increased DC migration to VDLNs (Fig. 2b). Vaccination and pre-conditioning with other CD4-dependent protein antigens also increased DC migration, suggesting that this may be a generalizable phenomenon (Extended Data Fig. 2). Subsequent studies performed in Td-treated mice demonstrated that only selective depletion of $CD4^+$ T cells abrogated the increase in DC migration (Fig. 2c). The effect of enhanced migration was also transferable to naive mice administered Td-activated $CD4^+$ T cells (Fig. 2d).

In patients with GBM randomized to unilateral Td pre-conditioning (Fig. 2e) and in mice (Fig. 2f), we observed an increased uptake of ^{111}In-labelled DCs in bilateral lymph nodes, suggesting that Td pre-conditioning increased DC migration through systemic mediators. Subsequent experiments revealed that Td-activated $CD4^+$ T cells administered systemically in naive mice were also sufficient to increase bilateral DC migration (Extended Data Fig. 3). Vaccine site pre-conditioning with unpulsed DCs or TNF-α (ref. 8) only increased DC migration ipsilaterally (Extended Data Fig. 4a, b).

On the basis of our observations that Td recall responses could induce bilateral DC migration and that systemic administration of Td-activated $CD4^+$ T cells was sufficient to recapitulate the increased DC migration, we sought to examine the induction of CD4-dependent inflammatory mediators in the serum of patients and mice after a recall response with Td pre-conditioning. CCL3 was the only chemokine or cytokine to be increased in both patients and mice and had the greatest fold increase of all chemokines in the serum of both after Td pre-conditioning (Fig. 3a and Extended Data Fig. 5a–d).

To identify the site of the CCL3 production, we assayed the pre-conditioning sites in mice and found high concentrations of this chemokine only unilaterally at the site of Td pre-conditioning (Extended Data Fig. 6a). Subsequent experiments showed that CCL3 upregulation in the skin was dependent on the induction of the Td recall response (Extended Data Fig. 6b) and was significantly reduced by $CD4^+$ T-cell depletion (Extended Data Fig. 6c). Induction of CCL3 by Td pre-conditioning remained increased over time compared to mice lacking Td recall responses (Extended Data Fig. 6d).

To evaluate the importance of CCL3 in mediating DC trafficking to VDLNs *in vivo*, we immunized and boosted *Ccl3*$^{-/-}$ mice with Td as described above and found that the migration of injected DCs to VDLNs in *Ccl3*$^{-/-}$ mice was significantly lower than in wild-type Td pre-conditioned mice (Fig. 3b, top). Endogenous migration experiments revealed that resident Langerhans cells also did not migrate as efficiently in *Ccl3*$^{-/-}$ hosts after Td pre-conditioning (Extended Data Fig. 7). To address the possibility that Td priming may have failed in *Ccl3*$^{-/-}$ mice owing to some earlier role of CCL3, we compared the CD4 T-cell-dependent immune responses to Td in both wild-type and *Ccl3*$^{-/-}$ hosts and found no differences in the ability of these two strains to mount anti-tetanus immune responses after Td priming and boosting (Extended Data Fig. 8).

Our studies demonstrated that $CD4^+$ T cells activated by the Td recall response were sufficient to induce increased DC migration in naive mice (Fig. 2d). However, Td-activated $CD4^+$ T cells could not rescue the limited DC migration in *Ccl3*$^{-/-}$ hosts indicating that activated T cells were necessary, but not sufficient to increase DC migration (Fig. 3b, bottom). Exogenous administration of CCL3 could rescue the limited

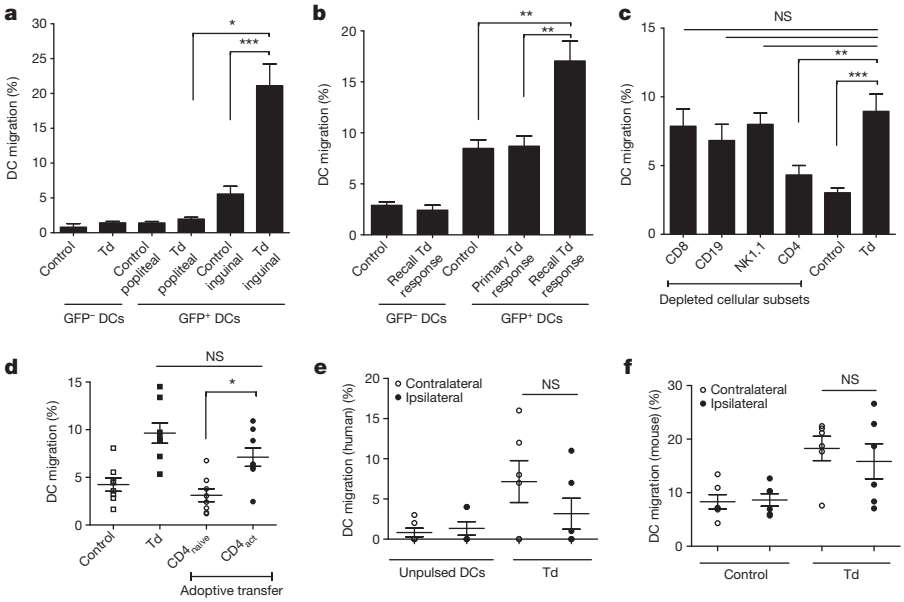

Figure 2 | Td recall response activates $CD4^+$ T cells to increase DC migration to VDLNs. **a**, Control inguinal ($n = 5$ mice) versus Td inguinal ($n = 5$ mice); two sample *t*-test, $P = 0.0001$; Td popliteal ($n = 5$ mice) versus Td inguinal, paired *t*-test, $P = 0.014$. **b**, Mice primed and boosted with saline (primary Td, $n = 6$) or Td (control and recall Td, $n = 6$) with Td (primary and recall Td) or saline (control) pre-conditioning; one-way analysis of variance (ANOVA), $P = 0.004$; post-hoc Tukey *t*-test, control versus recall Td, $P = 0.006$; primary Td versus recall Td, $P = 0.011$. **c**, DC migration in depleted Td-immunized mice ($n = 5$); one-way ANOVA, $P < 0.0001$; post-hoc Tukey *t*-test, Td versus CD4, $P = 0.005$; Td versus CD8, CD19 or NK1.1, $P > 0.05$. **d**, DC migration after $CD4^+$ transfer ($n = 4$ mice); one-way ANOVA, $P < 0.0001$; post-hoc Tukey *t*-test, Td-activated $CD4^+$ T cells ($CD4_{act}$) versus $CD4_{naive}$, $P < 0.05$; control versus $CD4_{naive}$, $P > 0.05$; Td versus $CD4_{act}$, $P > 0.05$. **e**, Patient (**e**) and mouse (**f**) iLN ipsilateral ($n = 6$) and contralateral ($n = 6$) to pre-conditioning; paired *t*-test, $P = 0.28$ (**e**) and $P = 0.37$ (**f**). **a**–**d** and **f** are representative of four experiments; mean ± s.e.m. Data in **a**–**d** denote biological replicates of individual right and left iLN or lymph nodes ipsilateral to Td/saline for popliteal and GFP^- groups.

©2015 Macmillan Publishers Limited. All rights reserved

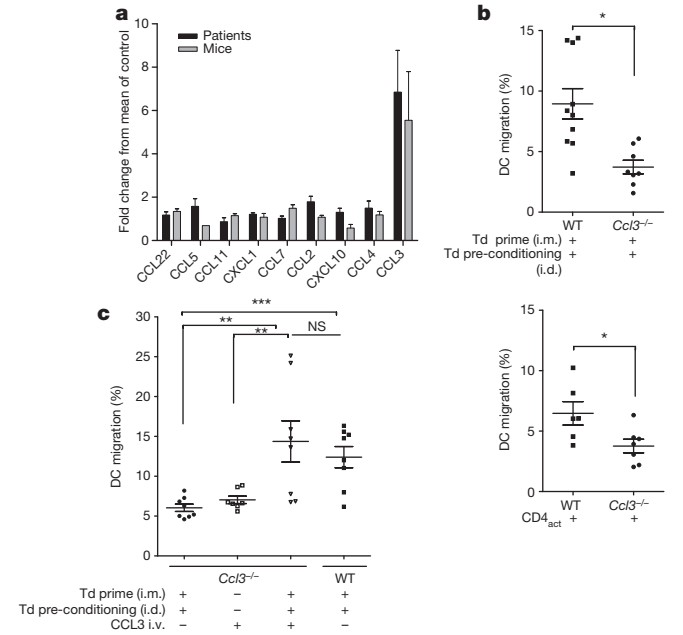

Figure 3 | Td recall responses and induced CCL3 cooperate to facilitate DC migration to VDLNs. **a**, Serum CCL3 fold increase over non-Td cohorts (patient, $n = 6$; mouse, $n = 8$ biological replicates); signed-rank test, $P = 0.031$ and $P = 0.039$. **b**, Top, DC migration in wild-type (WT) ($n = 5$) versus *Ccl3*$^{-/-}$ ($n = 4$) mice; two sample *t*-test, $P = 0.023$. Bottom, Td-activated CD4^{+} transfer in *Ccl3*$^{-/-}$ hosts ($n = 4$ mice); two sample *t*-test, $P = 0.029$. **c**, CCL3 and Td recall responses rescue migration ($n = 4$ mice); one-way ANOVA, $P < 0.0001$; post-hoc Tukey *t*-test, *Ccl3*$^{-/-}$ Td plus Td i.d. and CCL3 i.v. versus *Ccl3*$^{-/-}$ Td plus Td i.d. and versus *Ccl3*$^{-/-}$ plus CCL3 i.v., $P = 0.007$ and $P = 0.001$, respectively. Data in **b** and **c** denote biological replicates of individual right and left iLNs. Representative of three experiments; mean ± s.e.m. i.d., intradermal; i.m., intramuscular; i.v., intravenous.

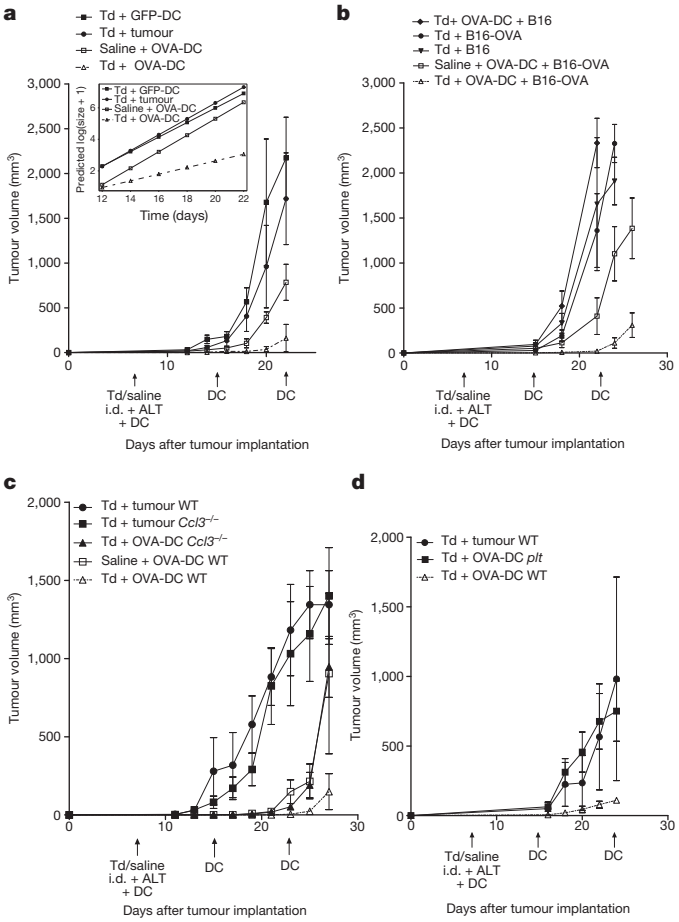

Figure 4 | Td pre-conditioning improves responses in tumour-bearing mice. **a**, Inset, transformed growth curves, mixed linear effects model. Pairwise comparisons of regression line slopes (*F*-test, $P < 0.0001$). Day 22 volume (Td plus OVA-DC versus Td plus GFP-DC, two sample *t*-test, $P = 0.002$; $n = 7$). **b**, Antigen-specific responses with Td pre-conditioning. Day 15 volume (all groups, *F*-test, $P = 0.016$; pairwise Tukey *t*-tests, Td plus OVA-DC and B16-OVA ($n = 7$) versus Td plus OVA-DC and B16 ($n = 5$), $P = 0.0004$; Td plus OVA-DC and B16-OVA versus saline plus OVA-DC and B16-OVA ($n = 6$), $P = 0.0002$). Day 22 volume (Td plus OVA-DC and B16-OVA versus Td plus OVA-DC and B16, two sample *t*-test, $P < 0.0001$). **c**, Tumour growth in *Ccl3*$^{-/-}$ mice. Day 11 volume (all groups, *F*-test, $P = 0.005$). Day 27 volume (Td plus OVA-DC WT versus Td plus OVA-DC *Ccl3*$^{-/-}$, two sample *t*-test, $P = 0.042$; $n = 8$). **d**, Anti-tumour responses in *plt* mice. Day 16 volume (all groups, *F*-test, $P = 0.004$). Day 24 volume (Td plus OVA-DC *plt* ($n = 7$) versus Td plus OVA-DC WT ($n = 6$), two sample *t*-test, $P < 0.05$). Data in **a**–**d** are representative of three experiments; mean ± s.e.m. ALT, autologous lymphocyte transfer.

DC migration in *Ccl3*$^{-/-}$ mice, but only when the Td recall responses were induced (Fig. 3c), indicating that the ability of Td pre-conditioning to increase DC migration to VDLNs was dependent on both CD4^{+} recall responses and host-derived CCL3.

Alterations in CCL21 expression along the lymphatic endothelium in the skin take place in the context of inflammation and have been associated with increased DC migration[8]. After Td pre-conditioning, higher levels of CCL21 in collected skin sites were detected in Td-treated wild-type mice compared to *Ccl3*$^{-/-}$ mice, and exogenous administration of CCL3 rescued the diminished levels of CCL21 at the vaccine sites of *Ccl3*$^{-/-}$ mice only in the context of Td recall responses (Extended Data Fig. 9a), which paralleled the requirement of host CCL3 and Td recall responses for increased DC migration. Furthermore, Td pre-conditioning resulted in an increase in CCL21 within inguinal lymph nodes both ipsilateral and contralateral to the side of Td pre-conditioning (Extended Data Fig. 9b). Although lymph nodes contain high basal amounts of CCL21, we found CCL21 levels in bilateral inguinal lymph nodes of Td-treated *Ccl3*$^{-/-}$ mice to be lower than that of wild-type mice. Meanwhile, reconstitution of CCL3 back into *Ccl3*$^{-/-}$ mice in conjunction with the induction of Td recall responses markedly increased the expression of CCL21 in VDLNs (Extended Data Fig. 9c).

The apparent increase in progression-free and overall survival for Td treated-patients prompted us to determine whether Td pre-conditioning could inhibit tumour growth in a mouse subcutaneous tumour model in which B16F10 melanoma cells expressed OVA (B16-OVA). Pairwise comparisons revealed that tumour growth in Td plus OVA-DC mice was significantly delayed (Fig. 4a) in an antigen-dependent manner (Fig. 4b). Td pre-conditioning in *Ccl3*$^{-/-}$ mice, as expected, was unable to inhibit tumour growth (Fig. 4c). Similarly, *plt* (paucity of lymph node T cell) mice, which lack expression of CCL21 in the lymph nodes[17], also failed to suppress tumour growth (Fig. 4d), indicating that Td-enhancement of OVA-DC vaccines also required intact CCL21 expression in the host.

Results from our trial seem to demonstrate that the modulation of CMV-specific DCs with Td pre-conditioning increases their migratory capacity and may improve clinical outcomes in patients with GBM. Corroborating studies in mice support these claims and underline CCL3 as a novel and important mediator of increased DC migration to VDLNs, in addition to its described roles in DC precursor mobilization to peripheral sites of inflammation[18,19] and in guiding naive CD8^{+} localization to sites of DC–CD4^{+} interactions in lymph nodes[20]. Our preclinical findings suggest that increased DC migration was only observed in the context of host CCL3 and Td recall responses. Similarly, we observed a slight increase in CCL21 skin and bilateral VDLN levels in the context of both host CCL3 and Td recall, which may have a role in DC homing to local lymph nodes. However, owing to the already high basal amount

©2015 Macmillan Publishers Limited. All rights reserved

of CCL21 chemokine in draining lymph nodes, it is possible that additional factors such as interactions between host CCL3 and $CD4^+$ recall T cells are the predominant contributors to the increased DC accumulation in VDLNs. Our findings also suggest that DC migration should be further investigated as a predictive biomarker for immunotherapy studies.

Online Content Methods, along with any additional Extended Data display items and Source Data, are available in the online version of the paper; references unique to these sections appear only in the online paper.

Received 6 December 2013; accepted 13 February 2015.
Published online 11 March 2015.

1. Steinman, R. M. & Banchereau, J. Taking dendritic cells into medicine. *Nature* **449,** 419–426 (2007).
2. Palucka, A. K. *et al.* Spontaneous proliferation and type 2 cytokine secretion by CD4+T cells in patients with metastatic melanoma vaccinated with antigen-pulsed dendritic cells. *J. Clin. Immunol.* **25,** 288–295 (2005).
3. Palucka, A. K. *et al.* Single injection of $CD34^+$ progenitor-derived dendritic cell vaccine can lead to induction of T-cell immunity in patients with stage IV melanoma. *J. Immunother.* **26,** 432–439 (2003).
4. Palucka, A. K. *et al.* Dendritic cells loaded with killed allogeneic melanoma cells can induce objective clinical responses and MART-1 specific $CD8^+$ T-cell immunity. *J. Immunother.* **29,** 545–557 (2006).
5. Palucka, K. & Banchereau, J. Cancer immunotherapy via dendritic cells. *Nature Rev. Cancer* **12,** 265–277 (2012).
6. Liau, L. M. *et al.* Dendritic cell vaccination in glioblastoma patients induces systemic and intracranial T-cell responses modulated by the local central nervous system tumor microenvironment. *Clin. Cancer Res.* **11,** 5515–5525 (2005).
7. Yu, J. S. *et al.* Vaccination with tumor lysate-pulsed dendritic cells elicits antigen-specific, cytotoxic T-cells in patients with malignant glioma. *Cancer Res.* **64,** 4973–4979 (2004).
8. Martin-Fontecha, A. *et al.* Regulation of dendritic cell migration to the draining lymph node: impact on T lymphocyte traffic and priming. *J. Exp. Med.* **198,** 615–621 (2003).
9. Dziurzynski, K. *et al.* Consensus on the role of human cytomegalovirus in glioblastoma. *Neuro Oncol.* **14,** 246–255 (2012).
10. Ranganathan, P., Clark, P. A., Kuo, J. S., Salamat, M. S. & Kalejta, R. F. Significant association of multiple human cytomegalovirus genomic Loci with glioblastoma multiforme samples. *J. Virol.* **86,** 854–864 (2012).
11. Mitchell, D. A. *et al.* Sensitive detection of human cytomegalovirus in tumors and peripheral blood of patients diagnosed with glioblastoma. *Neuro Oncol.* **10,** 10–18 (2008).
12. Cobbs, C. S. *et al.* Human cytomegalovirus infection and expression in human malignant glioma. *Cancer Res.* **62,** 3347–3350 (2002).
13. Myers, M. G., Beckman, C. W., Vosdingh, R. A. & Hankins, W. A. Primary immunization with tetanus and diphtheria toxoids. Reaction rates and immunogenicity in older children and adults. *J. Am. Med. Assoc.* **248,** 2478–2480 (1982).
14. Stupp, R. *et al.* Radiotherapy plus Concomitant and Adjuvant Temozolomide for Glioblastoma. *N. Engl. J. Med.* **352,** 987–996 (2005).
15. Curran, W. J. Jr. *et al.* Recursive partitioning analysis of prognostic factors in three Radiation Therapy Oncology Group malignant glioma trials. *J. Natl Cancer Inst.* **85,** 704–710 (1993).
16. Gorlia, T. *et al.* Nomograms for predicting survival of patients with newly diagnosed glioblastoma: prognostic factor analysis of EORTC and NCIC trial 26981–22981/CE.3. *Lancet Oncol.* **9,** 29–38 (2008).
17. Nakano, H. & Gunn, M. D. Gene duplications at the chemokine locus on mouse chromosome 4: multiple strain-specific haplotypes and the deletion of secondary lymphoid-organ chemokine and EBI-1 ligand chemokine genes in the plt mutation. *J. Immunol.* **166,** 361–369 (2001).
18. Zhang, Y. *et al.* Mobilization of dendritic cell precursors into the circulation by administration of MIP-1α in mice. *J. Natl Cancer Inst.* **96,** 201–209 (2004).
19. He, S. *et al.* MIP-3α and MIP-1α rapidly mobilize dendritic cell precursors into the peripheral blood. *J. Leukoc. Biol.* **84,** 1549–1556 (2008).
20. Castellino, F. *et al.* Chemokines enhance immunity by guiding naive $CD8^+$ T cells to sites of $CD4^+$ T cell-dendritic cell interaction. *Nature* **440,** 890–895 (2006).

Acknowledgements The authors thank the staff who supported this study, including R. Schmittling, P. Norberg, W. Xie, P. Healy, D. Lally-Goss, S. McGehee-Norman, B. Perry, S. Snipes and R. Edward Coleman. This work was supported by grants from the National Institutes of Health (NIH) National Institute of Neurological Disorders and Stroke Specialized Program of Research Excellence in brain cancer (P50-CA108786, D.D.B. and J.H.S.) and SRC on Primary and Metastatic Tumors of the CNS (P50-NS20023, D.D.B. and J.H.S.) as well as NIH RO1 (R01-CA177476-01, J.H.S.; R01-NS067037, R01-CA134844, D.A.M.) and P01 (P01-CA154291-01A1, D.D.B. and J.H.S.) funding sources. Additional support is from the National Brain Tumor Society (D.A.M. and J.H.S.), the American Brain Tumor Association (D.A.M. and J.H.S.), Accelerate Brain Cancer Cure Foundation Young Investigator's Award (D.A.M.), The Kinetics Foundation, (J.H.S.) Ben and Catherine Ivy Foundation (J.H.S.), and in part by Duke University's Clinical & Translational Science Awards grant 1UL2 RR024128-01 from the National Institutes of Health National Center for Research Resources.

Author Contributions D.A.M., G.E.A. and J.H.S. jointly conceived and implemented the clinical study; D.A.M. and K.A.B. jointly designed early DC migration studies in mice. K.A.B. conceived and designed the remainder of the mouse research; A.D., A.H.F., H.S.F., R.E.M., D.A.R., J.J.V., D.D.B. and J.H.S. were responsible for provision of clinical study resources, materials and patient access. S.K.N., E.A.R. and G.E.A. prepared human samples and conducted human *in vitro* experiments; K.A.B. performed all preclinical experiments and patient analyses; M.-N.H. provided additional support for preclinical experiments. D.A.M., K.A.B., M.D.G., K.L.C., E.A.R., G.E.A. and J.H.S. performed data analysis and interpretation; J.E.H. and A.C. provided statistical support for design and analysis of human and mouse studies. D.A.M., D.D.B. and J.H.S. contributed laboratory reagents and tools; and D.A.M., K.A.B., M.D.G., K.L.C. and J.H.S. wrote the paper. All authors gave their final approval to the manuscript.

Author Information Reprints and permissions information is available at www.nature.com/reprints. The authors declare competing financial interests: details are available in the online version of the paper. Readers are welcome to comment on the online version of the paper. Correspondence and requests for materials should be addressed to J.H.S. (john.sampson@duke.edu) or D.A.M. (duane.mitchell@neurosurgery.ufl.edu).

©2015 Macmillan Publishers Limited. All rights reserved

METHODS

Patient selection, demographics and clinical protocol. The clinical protocol and informed consent were approved by the US Food and Drug Administration and Institutional Review Board at Duke University. Adults with a newly diagnosed World Health Organization (WHO) grade IV GBM, who had a gross total resection and residual radiographic contrast enhancement on post-resection magnetic resonance imaging (MRI) not exceeding 1 cm in diameter in two perpendicular axial planes, and a Karnofsky performance scale score of ≥80, were eligible for the clinical study (FDA - IND-BB-12839, Duke IRB Pro00003877, NCT00639639). Histopathology of all specimens was initially read as GBM, but this diagnosis was re-confirmed by a second board-certified neuropathologist. Histological diagnosis included immunohistochemistry for MGMT protein expression. Benign endothelial cells staining positive for MGMT served as the internal control[21]. *MGMT* promoter methylation was performed by PCR. On the basis of published reports showing high expression of CMV viral proteins in >90% of GBM tumours[9–12], we elected not to include pp65 staining of tumour tissue as an eligibility criterion for this trial. All 13 patients on study received a gross total resection defined as >90% with residual contrast enhancement of $<1\ cm^2$, and steroid doses could not exceed 2 mg day^{-1} of dexamethasone. No patients received intensity-modulated radiation therapy or had 5-aminolevulinic acid dye used during resection. Thereafter, all patients completed a 6-week course of conformal external beam radiotherapy to a dose of 60 Gy with concurrent temozolomide at a targeted daily dose of 75 mg m^{-2} day^{-1}. After completion of standard therapy, all patients underwent an MRI for evidence of progressive disease. Those with evidence of progressive disease or required steroid therapy in excess of physiological levels at the time of vaccination were replaced. A total of 13 patients were enrolled and randomized before the first cycle of standard-of-care 5-day TMZ (200 mg m^{-2} day^{-1}), but one progressed before randomization. For each vaccine, 2×10^7 mature pp65 RNA-pulsed DCs in 0.4 ml of saline were given intradermally in the groin. The first vaccination occurred on day 21 ± 2 of TMZ cycle 1. Although some patients ($n = 5$) were also randomized to receive an autologous lymphocyte transfer, those patients did not show a significant improvement in progression-free or overall survival. Patients given autologous lymphocytes were additionally administered 3×10^7 cells kg^{-1} intravenously with acetaminophen (650 mg per os (po)) and Benadryl (25–50 mg po) given 30–60 min before infusion. The first three DC vaccines were given bi-weekly, and, at vaccine 4, patients were randomized to Td or unpulsed autologous DCs and received ^{111}In-labelled DCs for migration studies. Vaccine 4 and additional monthly vaccines until tumour progression occurred on day 21 ± 2 of successive TMZ cycles. A minimum of six cycles of adjuvant TMZ were required as per standard-of-care and continuation was at the discretion of the treating neurooncologist. Patients were monitored for treatment-related toxicity, and none of the patients experienced any vaccine or Td-related adverse events.

Human autologous DC generation for vaccination and production of pp65-LAMP/A64 mRNA. DCs were generated using the method described previously[22], and after collection the cells were frozen and assessed for contamination and lineage purity as previously published[23]. The 1.932-kilobase (kb) pp65 full-length cDNA insert was obtained from B. Britt and RNA was generated and transfected as previously reported[22].

Human DC migration studies. DC migration studies were done at the fourth vaccination. Patients were randomized by side to have one inguinal vaccination site pre-treated with either 1×10^6 unpulsed DCs or Td toxoid (1 flocculation unit (Lf)). Saline was administered on the contralateral side. Vaccination site pretreatment was done 6–24 h before DC vaccination. DCs were labelled with 10 μCi per 1×10^7 DC with ^{111}In (GE Healthcare) and divided equally in the two sites. Gamma camera images (GE Infinia Hawkeye) were taken immediately after injection and at 24 and 48 h after injection to compare ^{111}In-labelled DC migration from the inguinal injection sites to the inguinal lymph nodes.

Progression-free and overall survival. The more recent response evaluation criteria in solid tumours (RECIST criteria) judge progression by measuring the longest one-dimensional diameter and determine progression by a 20% increase in this diameter[24]. Once progression is detected on MRI, other imaging modalities such as positron emission tomography and a stereotactic brain biopsy of the enhancing region are incorporated to aid in determining progression. A stereotactic brain biopsy or resection demonstrating recurrence defines clinical progression. Progression-free survival was defined as the time until radiographic or clinical progression and was censored at the last follow-up if the patient remained alive without disease progression. Overall survival was defined as the time until death and was censored at the last follow-up if the patient remained alive at the time of analysis. Progression-free and overall survival for all patients were calculated from both the time of surgery and from randomization to vaccine site pre-conditioning.

Mice. All animal experiments were performed according to Duke University Institutional Animal Care and Use Committee-approved protocols. Female C57BL/6 wild-type, OT-I transgenic mice, *Ccl3*$^{-/-}$, and red fluorescent protein (RFP) and green fluorescent protein (GFP) transgenic mice (ubiquitin promoter) were obtained from the Jackson Laboratory and were bred under pathogen-free conditions at Duke University Medical Center. The *plt* strain was provided by M.D.G. and maintained at Duke University Medical Center. All mice were bred under pathogen-free conditions at Duke University Medical Center.

Generation of mouse bone marrow-derived DCs, electroporation and phenotyping. Bone-marrow-derived DCs were generated from 6–8-week-old female C57BL/6 wild-type, RFP$^+$ or GFP$^+$ transgenic mice and pulsed with OVA RNA as previously described[25]. For phenotyping, anti-mouse phycoerythrin (PE)-conjugated CD11c (HL3), CD80 (16-10A1), CD86 (GL1), Ly-6G (1A8), MHC class II (I-A^b; AF6-120.1) and isotype controls (IgG1; G235-2356, IgG_{2a},κ; R35-95) were from BD Pharmingen. Cells were washed, resuspended in PBS and 2% FBS, incubated at 4 °C for 30 min, and washed again before use.

Vaccine site pre-conditioning and DC vaccination in mice. For Td immunization, female 6–8-week-old C57BL/6 mice received a primary intramuscular vaccine of Td toxoid (Sanofi Aventis; Decavac; 1 Lf, 100 μl) administered bilaterally into the quadriceps muscle (50 μl per leg). An intramuscular booster (0.5 Lf, 50 μl) was administered two weeks later. Vaccine site pre-conditioning with saline or Td toxoid (0.5 Lf) was given intradermally (i.d.) 2 weeks after the booster and randomized to the right or left groin site. Mouse IgG antibody responses to Td were measured by ELISA (Xpress Bio). Serum from immunized mice was collected 2 weeks after each immunization before the next booster vaccine. DCs were resuspended at 1×10^6 per 100 μl PBS (Gibco) and administered i.d. on both sides 0.8 cm from the groin crease 24 h after i.d. pre-conditioning. DCs injected in the groin ipsilateral to the Td pre-conditioning side were directly injected i.d. within the erythematous nodule produced by Td pre-conditioning. For recall response experiments using other protein antigen formulations, female 6–8-week-old C57BL/6 mice received a primary intramuscular vaccine of Prevnar 13 (Pfizer, Pneumococcal 13-valent conjugate vaccine, 1.32 μg, 100 μl) and Pedvax HIB (Merck, Haemophilus b conjugate vaccine, 1.5 μg, 100 μl) administered bilaterally into the quadriceps muscle (50 μl per leg). Vaccine site pre-conditioning with saline or the protein antigen (50 μl) was given i.d. 2 weeks later and randomized to the right or left groin site. DC vaccines were given 24 h later, and migration to lymph nodes was assessed 48 h later. As with Td pre-conditioning, DCs injected in the groin ipsilateral to the pre-conditioning side were directly injected i.d. within the erythematous nodule produced by those formulations. For comparisons of other pre-conditioning agents, female 6–8-week-old C57BL/6 mice received a unilateral dose of unpulsed, mature DCs (1×10^6 in 50 μl) or TNF-α (30 ng) administered i.d. at the groin site 24 h before DC vaccination. On the basis of the previous work using these pre-conditioning regimens, DC migration to bilateral inguinal lymph nodes was assessed 24 h later. For all other migration experiments, popliteal and inguinal lymph nodes were collected 48 h after DC vaccination and digested for flow cytometry. The percentage of migrating DCs was enumerated by gating on fluorescent DCs in wild-type VDLNs. DCs from wild-type (GFP$^-$ and RFP$^-$) mice as negative controls before gating on fluorescent DCs within VDLNs to account for background autofluorescent cells that may have appeared in the GFP channel. For *in vivo* DC migration, a sample size (three per group) was based on empirical evidence from previously published reports as the size necessary for adequate statistical analysis of lymph nodes sampled[26].

Depletion, adoptive transfer and CCL3 reconstitution. Female 6–8-week-old C57BL/6 mice were initially depleted of cellular subsets once daily (200 μg per mouse intraperitoneally) for 3 days before the first Td intramuscular immunization. Anti-mouse CD4 (GK1.5) and anti-CD8 (2.43) antibodies were purchased from American Type Culture Collection. Anti-mouse NK1.1 (PK136) and anti-CD19 (2D5) and control isotype depleting antibodies (IgG2a (2A3) and IgG2b (LTF-2)) were from BioXCell. Maintenance doses of depletion antibodies were administered at 3-day intervals (200 μg intraperitoneally) until vaccine site pre-conditioning with Td 2 weeks later. For adoptive transfer experiments, Td-activated CD4$^+$ T cells ($CD4_{act}$) were induced in donor female 6–8-week-old C57BL/6 mice. Mice were primed (1 Lf, 100 μl) and boosted (0.5 Lf, 50 μl) intramuscular with Td 2 weeks apart. Three days after the i.d. Td pre-conditioning, donor inguinal lymph nodes, skin injection sites, and spleens were collected and processed for negative isolation of CD4$^+$ T cells (Miltenyi Biotec). Complementary sites from naive mice were collected simultaneously and processed for negative isolation of CD4$^+$ T cells ($CD4_{naive}$). A final dose of 6×10^6 CD4$^+$ T cells were administered intravenously into recipient mice two days before i.d. vaccination with RFP$^+$ DCs. For CCL3 reconstitution in *Ccl3*$^{-/-}$ hosts, recombinant mouse CCL3 (R&D Systems) was administered intravenously into the tail vein (10 μg per mouse) 12 h before vaccination with RFP$^+$ DCs. *Ccl3*$^{-/-}$ mice that were Td-immune were given recombinant CCL3 12 h after Td pre-conditioning at the vaccine site.

Tumour implantation experiments. For tumour implantation experiments, B16F10-OVA cells were grown as previously published[27] and injected subcutaneously at a concentration of 2×10^5 cells in 200 μl of PBS in the flank of C57BL/6 mice 8 days before vaccine site pre-conditioning, the first intradermal vaccine of OVA RNA-pulsed

©2015 Macmillan Publishers Limited. All rights reserved

DCs, and autologous lymphocyte transfer (1:1 infusion of naive:OT-I OVA-specific T cells). Randomization of mice occurred after tumour inoculation before vaccine site pre-conditioning and the first DC vaccine first by compilation and then by random sorting into various treatment cages. Mice received two additional weekly vaccines of RNA-pulsed DCs on days 15 and 22. Ten days after tumour implantation, flank sites were monitored daily for tumour growth, and tumour size was measured every 2 days. Tumour volume (millimetres cubed) was calculated by the formula (length $\times$ width^2 $\times$ 0.52) in a perpendicular fashion. Mice were euthanized when ulceration occurred or when the tumour reached either 2 cm in any direction or 2,000 mm^3. Analysis of tumour growth focused on follow-up assessments before considerable dropout occurred. A logarithmic transformation yielded a linear relationship between tumour volume and time for all curves. A mixed effects linear model that accounted for correlation of measurements within a mouse was used to examine the relationship between time and log [tumour volume + 1]. No blinding was done for these animal studies.

Mouse tumour cell lines. The B16F10-OVA tumour cell line was a gift from R. Vile[27,28]. The B16F10 cell line was provided by I. Fidler[29]. Cell lines were tested for mycoplasma before use.

Mouse lymph node digestion and quantification of fluorescent and endogenous DCs. Lymph nodes were placed in 6-well culture plates containing 1 ml HBSS with Ca^{2+}/Mg^{2+} (Gibco), digested for 35 min at 37 °C with collagenase A (1 mg ml^{-1}; Roche) and DNaseI (0.2 mg ml^{-1}; Sigma-Aldrich) and 20 mM EDTA (Invitrogen) was added for 5 min at room temperature to stop the reaction[26]. Single-cell suspensions were prepared, cells were centrifuged (500*g* for 5 min) and resuspended in PBS with 2% FBS and stained with mouse allophycocyanin (APC)-conjugated CD11c (BD Pharmingen; HL3). For quantification of RFP$^+$ or GFP$^+$ counts in individual lymph nodes, samples were resuspended at an equal volume and 50 µl of counting beads (Invitrogen; 50,000 beads) were added to each sample. Cells were gated first on mouse CD11c$^+$ cells and then RFP$^+$ or GFP$^+$ cells, and absolute cell counts/lymph nodes were quantified using the following equation: RFP$^+$ or GFP$^+$ events $\times$ 50,000 beads/number of bead events. For endogenous DC migration experiments, cells were surface stained in PBS with 3% FBS, 10 mM EDTA, 5% normal mouse serum, 5% normal rat serum and 1% Fc Block (eBioscience; clone 93) and then intracellularly stained with anti-CD207 according to the manufacturer's protocol (BD Cytofix/Cytoperm Kit). The cells were analysed by BD LSRII flow cytometer with FlowJo software (Tree Star). FITC-conjugated anti-B220 (RA-3-6B2), Alexa Fluor 700-conjugated anti-Ly-6G (1A8), APC-Cy7-conjugated anti-CD11b (M1/70), V450-conjugated anti-Ly-6C (AL-21) are from BD Pharmingen. PE-conjugated anti-CD207 (eBioL31), PE-Cy5.5-conjugated anti-CD11c (N418), PE-Cy7-conjugated anti-CD8 (53.6.7), APC-conjugated anti-CD103 (2E7), eFluor 605NC-conjugated anti-CD45 (30-F11) and eFluor 650NC-conjugated anti-MHC class II (I-A/I-E) (M5/114.15.2) are from eBioscience. FITC-conjugated anti-CD3 (145-2C11) and anti-CD49b (DX5) are from BioLegend. The LIVE/DEAD Fixable Aqua Dead Cell Stain Kit is from Molecular Probes.

Serum cytokine and chemokine analysis. Peripheral blood was collected 24 h after vaccine site pre-conditioning before DC vaccination. For patients, blood was collected in 10 ml venous collection tubes (BD), allowed to clot, spun at 1,170*g* for 15 min, and serum was stored at −190 °C. For mice, blood was collected in microtainer tubes (BD) allowed to clot for 30 min, spun at 8,000*g* for 5 min, and serum was stored at −80 °C. Multiplex cytokine and chemokine kits were used for patient and mouse studies (cytokines and chemokines of interest for human, Affymetrix and Millipore: EPX080-10007-901, EPX010-12121-901, EPX010-12125-9, EPX010-10287-901, HCYTOMAG-60K-01 MDC; for mouse: Affymetrix and Millipore: EPX090-20821-901 ProcartaPlex 9 plex, MCYP3MAG-74K-01 MDC) following the manufacturer's instructions.

Expression of chemokines CCL3 and CCL21 in mice. Female 6–8-week-old C57BL/6 or *Ccl3*$^{-/-}$ mice were immunized with Td as described above. Twenty-four hours after Td pre-conditioning, both left and right skin sites and inguinal lymph nodes were collected. For protein isolation, skin and lymph node samples were placed in pre-loaded bead lysis Eppendorf tubes (Next Advance) containing RIPA buffer (Sigma) with protease inhibitor cocktail tablets (Mini Complete Protease Inhibitor Cocktail Tablets, Roche Applied Science). Homogenization was performed with the Bullet Blender at 4 °C. Supernatants were collected by centrifugation, and chemokines were quantified by ELISA. Quantikine kits (R&D Systems) were used for CCL3, and RayBiotech ELISA kits were used for CCL21. Corresponding samples were run for total protein concentration using the Bradford assay. CCL3 and CCL21 concentrations were normalized across samples and expressed as picograms or nanograms per milligram of total skin or lymph node protein.

Statistical analysis. Statistics were reviewed by biostatisticians and tested as described in figure legends. Cox proportional hazard models were used to evaluate DC migration and clinical outcomes. The log-rank test was used to compare Kaplan–Meier survival curves with censored patient data. For *in vivo* DC migration and VDLN studies, individual patient and mouse inguinal lymph nodes were treated as separate biological replicates, based on the underlying assumption that unilateral vaccine site pre-conditioning may preferentially affect local draining lymph nodes over non-draining sites. An unpaired two-sample Student's *t*-test was used for two-group comparisons. Paired *t*-tests were used for comparisons between lymph nodes in the same host. One-way ANOVA was used to assess differences among three or more groups with post-hoc Tukey *t*-tests for two-group comparisons. Wilcoxon rank sum analyses were conducted for pairwise comparisons in serum cytokine/chemokine panels. Signed rank tests were used to evaluate fold increase in chemokine levels. For tumour growth curves, a mixed effects linear model was employed using log-transformed curves and *F*-test for pairwise comparisons of regression line slopes and mean tumour volumes on the first day of detectable tumours (*y*-intercept). Repeated measures for calculation of slopes incorporated time between detectable tumour until considerable dropout occurred (maximal tumour size, ulceration, or death). Mean tumour volumes at final time points when the entire control cohort expired were compared between two groups using an unpaired two-sample student's *t* test. Asterisks indicate level of significance ($*P < 0.05$, $**P \leq 0.01$, $***P < 0.001$, $P > 0.05$ not significant). No statistical methods were used to predetermine sample size.

21. McLendon, R. E. *et al.* Immunohistochemical detection of the DNA repair enzyme O6-methylguanine-DNA methyltransferase in formalin-fixed, paraffin-embedded astrocytomas. *Lab. Invest.* **78,** 643–644 (1998).
22. Nair, S., Archer, G. E. & Tedder, T. F. Isolation and generation of human dendritic cells. **99,** 7.32:7.32.1–7.32.23 *Curr. Protoc. Immunol.* (2012).
23. Thurner, B. *et al.* Generation of large numbers of fully mature and stable dendritic cells from leukapheresis products for clinical application. *J. Immunol. Methods* **223,** 1–15 (1999).
24. Therasse, P. *et al.* New guidelines to evaluate the response to treatment in solid tumors. European Organization for Research and Treatment of Cancer, National Cancer Institute of the United States, National Cancer Institute of Canada. *J. Natl Cancer Inst.* **92,** 205–216 (2000).
25. Inaba, K., Swiggard, W. J., Steinman, R. M., Romani, N. & Schuler, G. Isolation of dendritic cells. *Curr. Protoc. Immunol.* **25,** 3.7:3.7.1–3.7.15 (2001).
26. Nakano, H. *et al.* Blood-derived inflammatory dendritic cells in lymph nodes stimulate acute T helper type 1 immune responses. *Nature Immunol.* **10,** 394–402 (2009).
27. Sanchez-Perez, L. *et al.* Potent selection of antigen loss variants of B16 melanoma following inflammatory killing of melanocytes in vivo. *Cancer Res.* **65,** 2009–2017 (2005).
28. Daniels, G. A. *et al.* A simple method to cure established tumors by inflammatory killing of normal cells. *Nature Biotechnol.* **22,** 1125–1132 (2004).
29. Fidler, I. J. Biological behavior of malignant melanoma cells correlated to their survival in vivo. *Cancer Res.* **35,** 218–224 (1975).

©2015 Macmillan Publishers Limited. All rights reserved

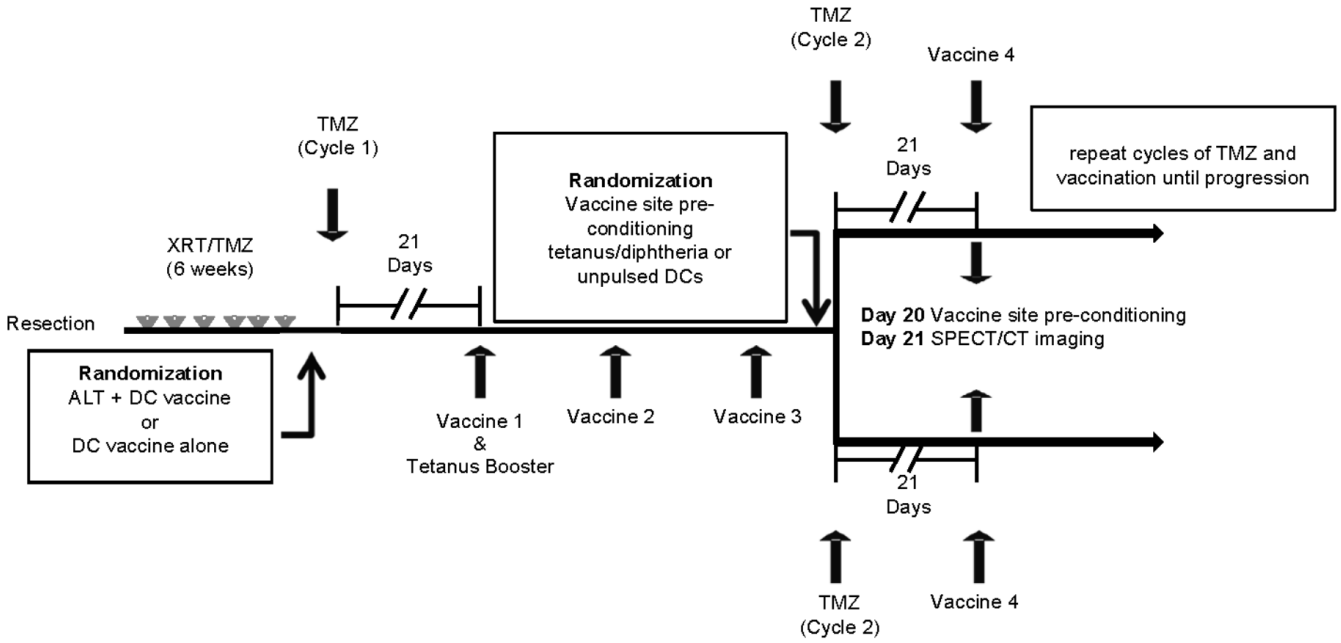

Extended Data Figure 1 | Schema of clinical trial. SPECT/CT, single photon emission computed tomography/computed tomography; TMZ, temozolomide; XRT, external beam radiotherapy.

©2015 Macmillan Publishers Limited. All rights reserved

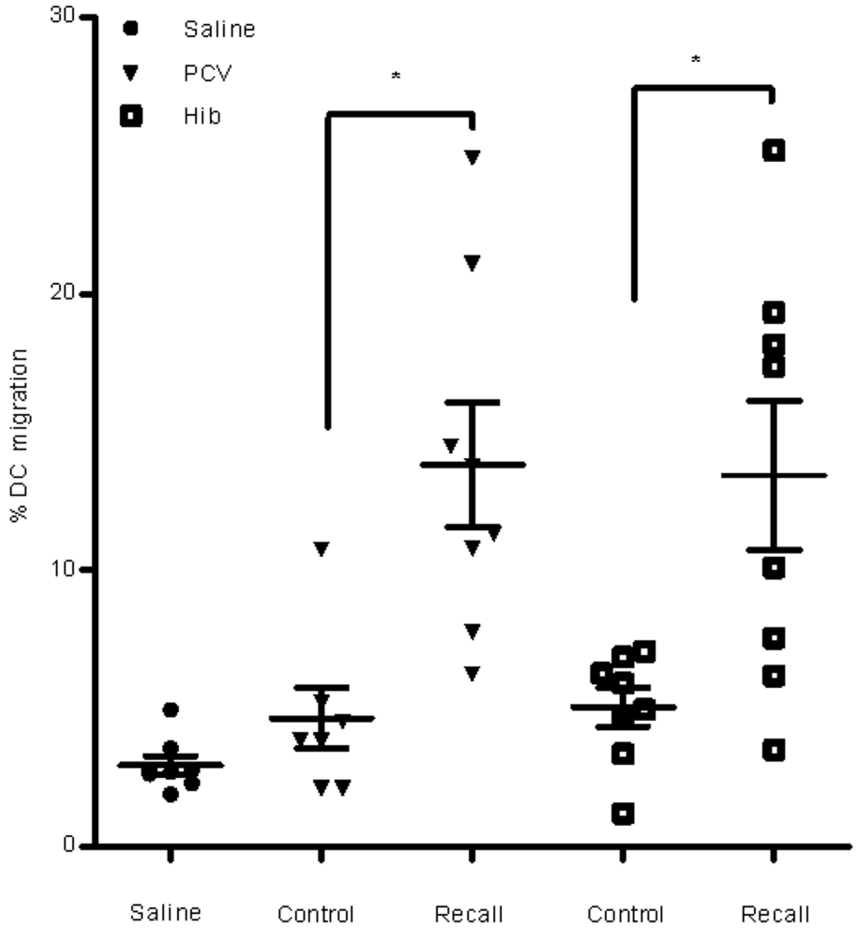

Extended Data Figure 2 | Recall responses induced by other CD4$^+$ T-cell-dependent protein antigens increase DC migration to VDLNs. Primary immunization and vaccine site pre-conditioning with CD4$^+$ T-cell-dependent protein antigens increase DC migration to VDLNs. Mice were immunized with either Haemophilus b conjugate (Hib) or pneumococcal 13-valent conjugate (PCV) intramuscularly, and 2 weeks later received vaccine site pre-conditioning with the recall antigen (recall) or saline (control). A separate cohort of mice received saline only throughout the immunization schedule (saline). Scatter plot shows biological replicates of individually processed right and left iLN per mouse (4 mice per group). Percentage migration of RFP$^+$ DCs to VDLNs; one-way ANOVA, $P < 0.0001$; post-hoc Tukey *t*-test, PCV control versus recall, $P < 0.05$, Hib control versus recall, $P < 0.05$. Representative of $n = 3$ experiments; mean ± s.e.m.

©2015 Macmillan Publishers Limited. All rights reserved

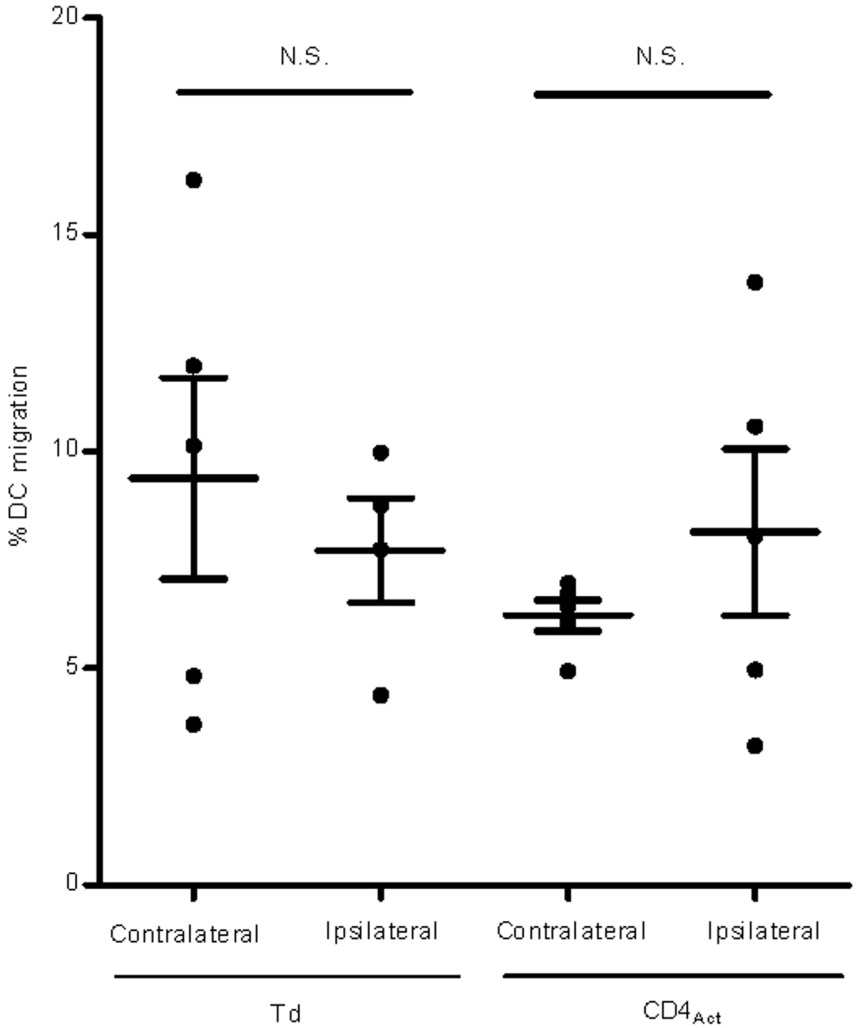

Extended Data Figure 3 | Bilateral migration of OVA-DCs after Td pre-conditioning or Td-activated CD4$^+$ T-cell transfer. Uptake of injected DCs to right and left iLNs 48 h after DC vaccination in Td-immune mice receiving Td pre-conditioning or naive mice administered Td-activated CD4$^+$ T cells. Scatter plot shows biological replicates of individually processed right and left iLN per mouse (5 mice per group). $CD4_{act}$ ipsilateral versus contralateral, paired *t*-test, $P = 0.41$. Representative of $n = 4$ experiments; mean ± s.e.m.

©2015 Macmillan Publishers Limited. All rights reserved

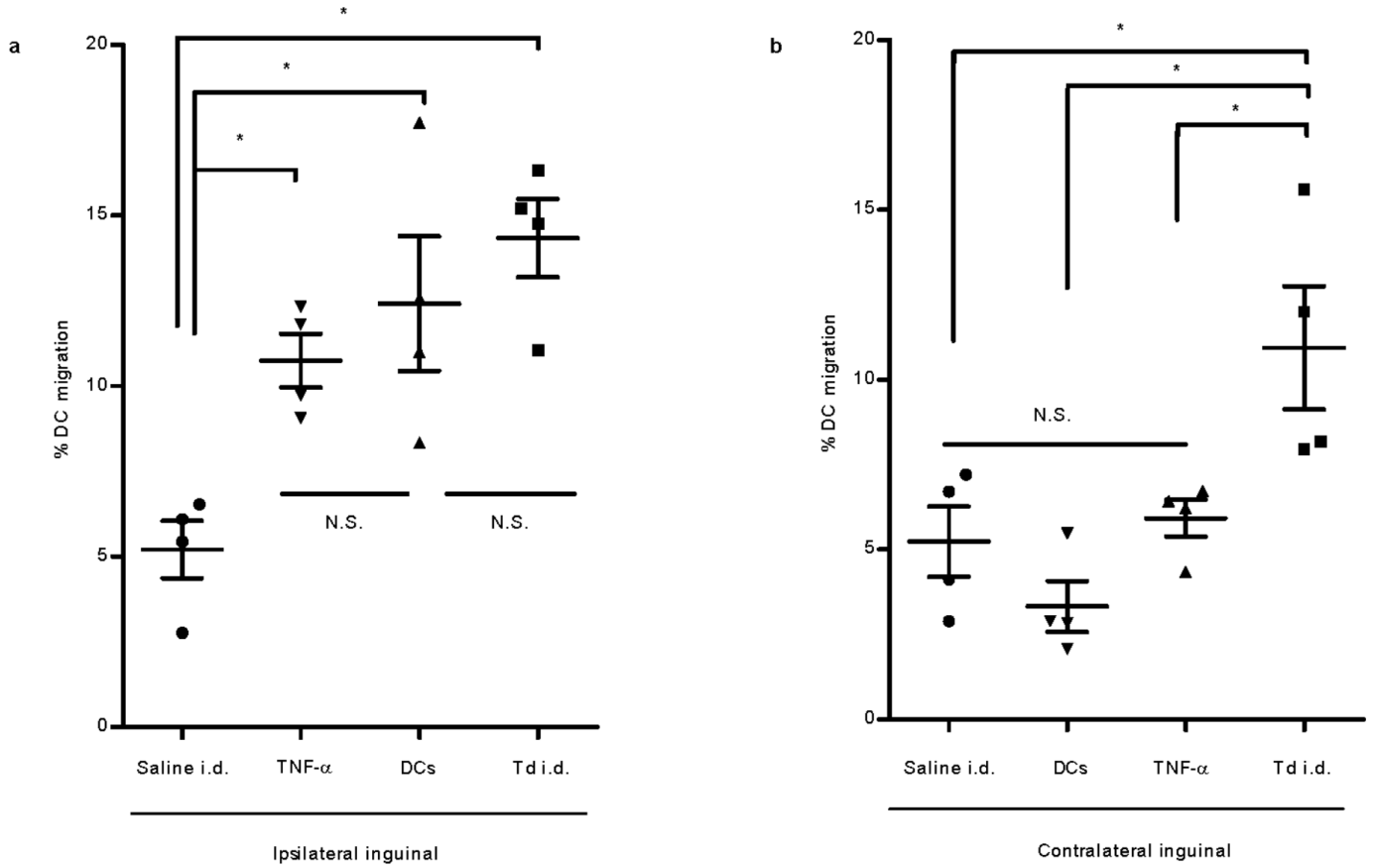

Extended Data Figure 4 | Unilateral pre-conditioning with unpulsed DCs or TNF-α results in increased DC homing to ipsilateral draining inguinal lymph nodes. Td-immune mice pre-conditioned with Td or saline before administration of OVA RNA-pulsed DC vaccine. Separate cohorts of naive mice received either 1×10^6 unpulsed DCs or 30 ng TNF-α on one side of the groin 24 h before the bilateral RFP^+ DC vaccine. DC migration was quantified 24 h after vaccination. **a**, DC migration to ipsilateral lymph nodes (one-way ANOVA, $P = 0.0018$; post-hoc Tukey *t*-test, saline i.d. versus Td i.d., $P = 0.007$; saline i.d. versus TNF-α, $P < 0.05$; saline i.d. versus DCs, $P < 0.05$; Td i.d. versus TNF-α, $P = 0.042$; DCs versus Td i.d. and DCs versus TNF-α, $P > 0.05$. **b**, DC migration to contralateral lymph nodes; one-way ANOVA, $P = 0.003$; post-hoc Tukey *t*-test, saline i.d. versus DCs or TNF-α, $P > 0.05$; Td i.d. versus TNF-α, DCs or saline i.d., $P < 0.05$. *n* values are biological replicates of individually processed right and left iLNs per mouse (4 mice per group). Representative of $n = 3$ experiments; mean ± s.e.m.

©2015 Macmillan Publishers Limited. All rights reserved

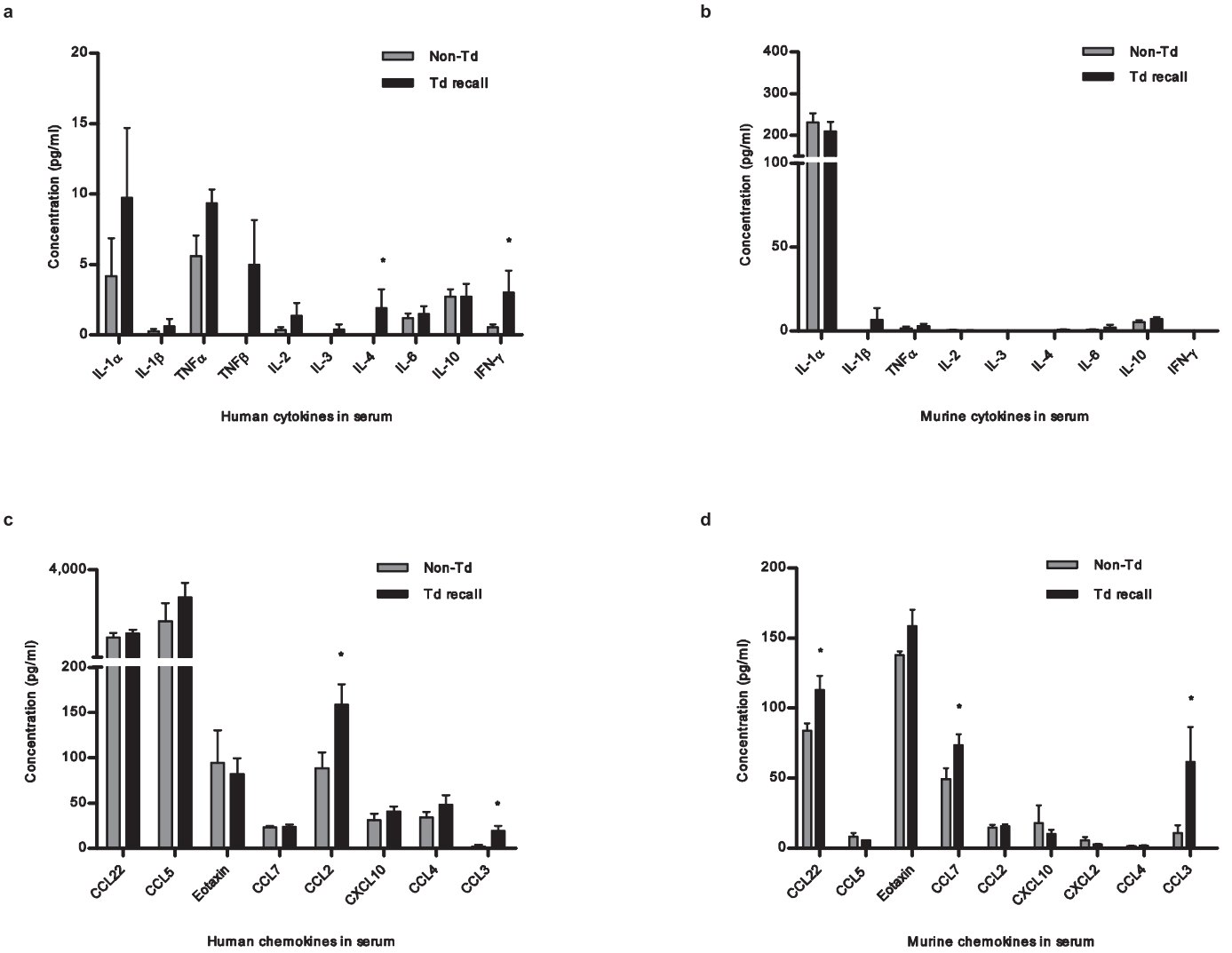

Extended Data Figure 5 | Serum cytokine and chemokine profile after Td pre-conditioning in patients and mice. **a**, Serum cytokine panel of patients following vaccine site pre-conditioning with Td or unpulsed DCs; Wilcoxon rank sum, IFN-γ and IL-4, $P < 0.05$ ($n = 6$ patients). **b**, Similar to **a** in mice; Wilcoxon rank sum, all comparisons, $P > 0.05$ (Td recall $n = 5$, non-Td $n = 6$). **c**, Patient serum chemokines after vaccine site pre-conditioning. Patient CCL2 and CCL3 in Td recall (Td, $n = 6$) versus non-Td (unpulsed DC, $n = 5$); one-way ANOVA and Wilcoxon rank sum, $P < 0.05$. **d**, Mouse CCL22, CCL7 and CCL3 in Td recall (Td, $n = 8$ mice) and non-Td (saline, $n = 8$ mice); one-way ANOVA and Wilcoxon rank sum, $P < 0.05$. For **a**–**d**, individual values represent biological replicates; mean ± s.e.m.

©2015 Macmillan Publishers Limited. All rights reserved

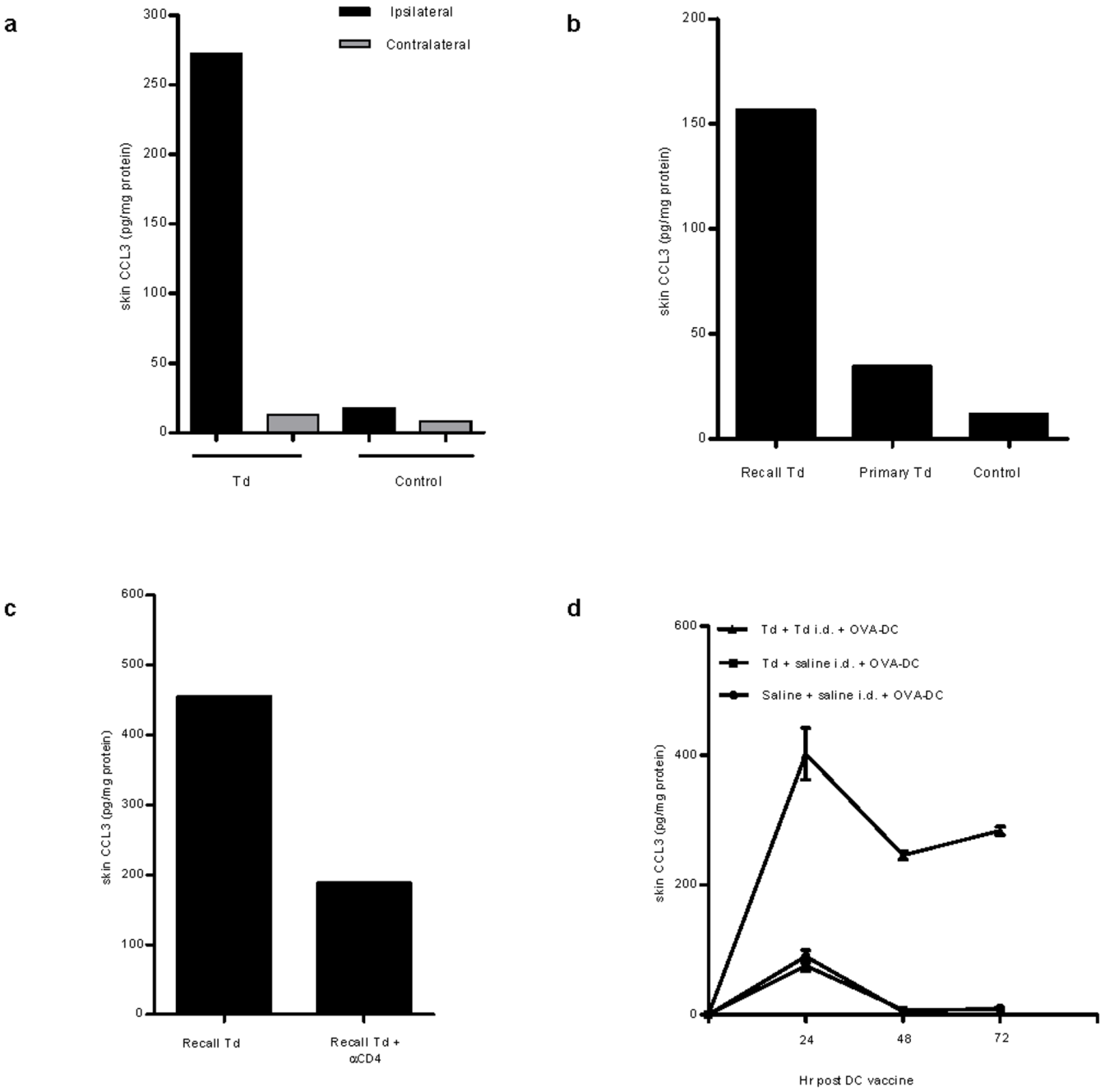

Extended Data Figure 6 | Td vaccine site pre-conditioning results in CCL3 upregulation in Td-immune hosts. **a**, CCL3 production in skin site after Td pre-conditioning (Td ipsilateral versus contralateral). Representative of four independent experiments. **b**, CCL3 production in skin after Td recall response. **c**, CCL3 induction at skin site is abrogated with previous host depletion of $CD4^+$ T cells. Bars in **a**–**c** represent CCL3 protein detected in skin sites from $n = 2$ mice with $n = 2$ technical replicates performed per mouse. **d**, CCL3 remains increased at the Td pre-conditioning site in the skin after DC vaccination (24, 48 and 72 h, one-way ANOVA, $P = 0.0001$, Td plus Td i.d. and OVA-DC versus Td plus saline i.d. and OVA-DC, and saline plus saline i.d. and OVA-DC, $P < 0.05$, post-hoc Tukey t-test). Individual values represent biological replicates from $n = 4$ mice; mean ± s.e.m.

©2015 Macmillan Publishers Limited. All rights reserved

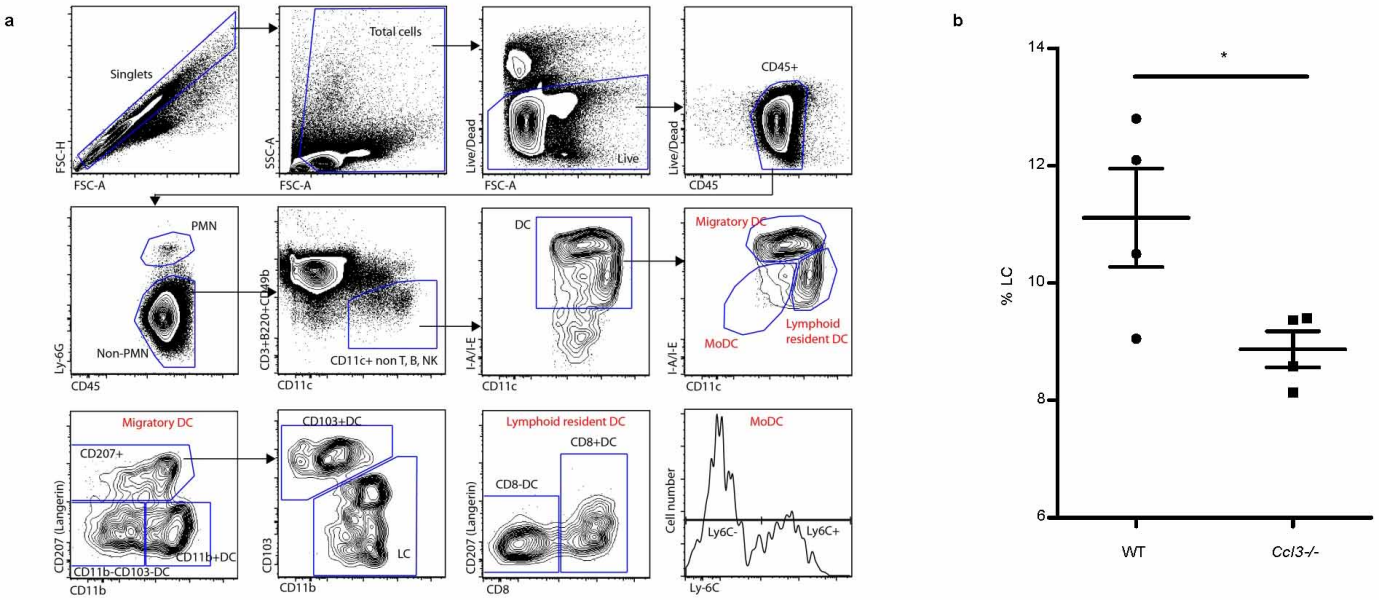

Extended Data Figure 7 | Migratory DC subsets in wild-type and *Ccl3*$^{-/-}$ mice after induction of Td recall responses. Both wild-type and *Ccl3*$^{-/-}$ mice were first immunized with Td and then challenged with Td pre-conditioning. Migration of endogenous DC subsets to inguinal lymph nodes contralateral to the site of Td pre-conditioning was assessed at days 4 and 8 after Td administration. **a**, Gating strategy used to quantify DC subsets in inguinal lymph nodes after skin pre-conditioning with Td. LC, Langerhans cells; MoDC, monocyte-derived DCs. **b**, Day-8 migration of LC population to non-draining inguinal lymph nodes in *Ccl3*$^{-/-}$ hosts is reduced in absence of CCL3; two-sample *t*-test, $P = 0.046$. Representative of three experiments. Individual values represent biological replicates from $n = 4$ mice; mean ± s.e.m.

©2015 Macmillan Publishers Limited. All rights reserved

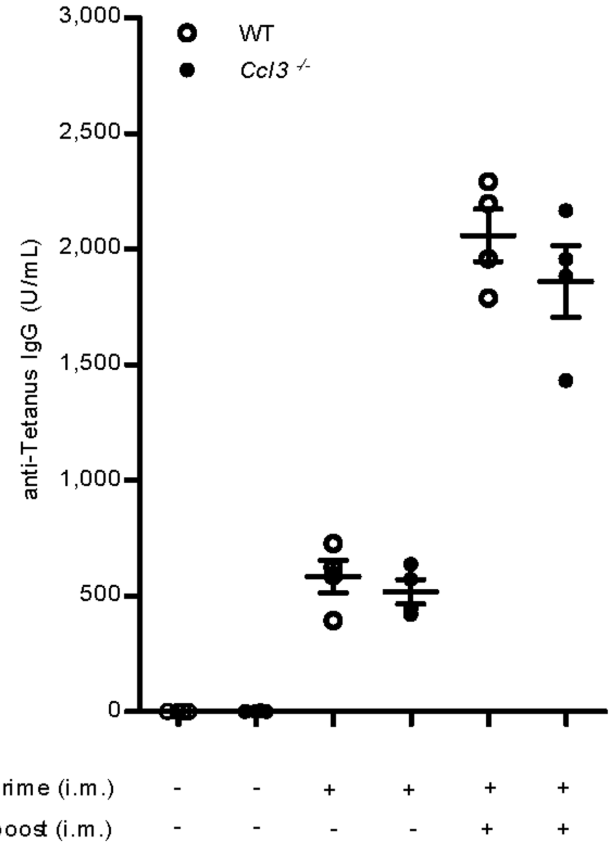

Extended Data Figure 8 | Anti-tetanus toxoid memory responses are induced and maintained in wild-type and *Ccl3*$^{-/-}$ mice throughout Td priming and boosting. Wild-type and *Ccl3*$^{-/-}$ mice primed and boosted with Td. Serum from immunized mice was collected 2 weeks after each immunization before the next booster vaccine (for each boosting phase, wild-type versus *Ccl3*$^{-/-}$, two-sample *t*-test, $P > 0.05$). i.m., intramuscular. Scatter plot showing averaged values from $n = 4$ mice with $n = 2$ technical replicates performed per mouse. Representative of three experiments; mean ± s.e.m.

©2015 Macmillan Publishers Limited. All rights reserved

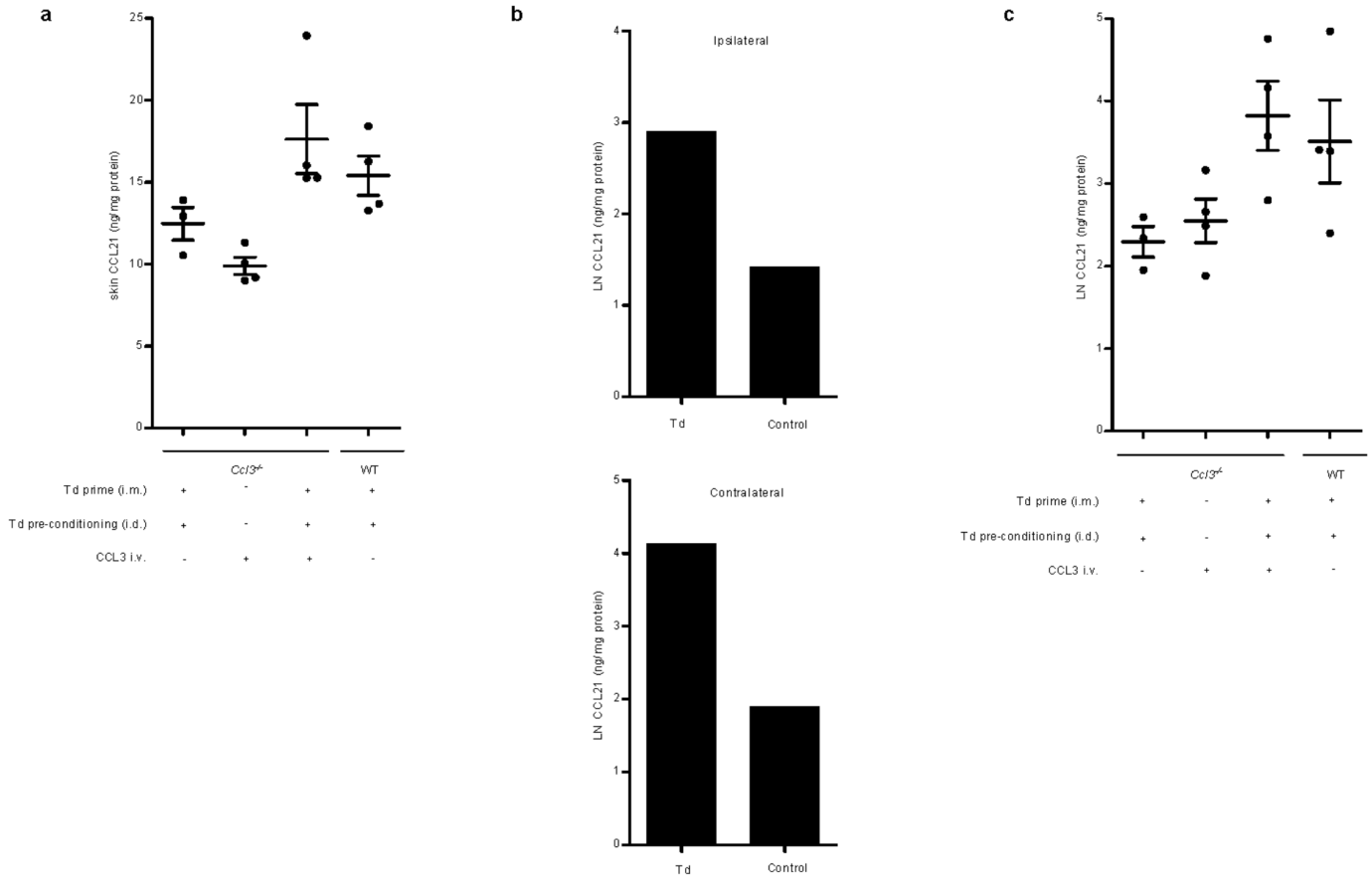

Extended Data Figure 9 | CCL21 levels in Td pre-conditioning skin sites and draining lymph nodes of wild-type and *Ccl3*$^{-/-}$ mice. **a**, CCL21 levels in skin site of *Ccl3*$^{-/-}$ hosts after induction of Td recall response and CCL3 administration. Mixed model accounting for within-mouse correlation of measurements, *F*-test, $P < 0.001$; pairwise comparisons, WT Td plus Td i.d. ($n = 4$) versus *Ccl3*$^{-/-}$ Td plus Td i.d. ($n = 3$), $P = 0.049$; *Ccl3*$^{-/-}$ Td plus Td i.d. and CCL3 i.v. ($n = 4$) versus *Ccl3*$^{-/-}$ Td plus Td i.d. and versus *Ccl3*$^{-/-}$ plus CCL3 i.v. ($n = 4$), $P = 0.044$ and $P = 0.0045$, respectively. Scatter plot shows averaged values with $n = 2$ technical replicates performed per mouse. **b**, Bilateral iLN CCL21 levels in wild-type mice after Td recall with skin site pre-conditioning. Bars represent CCL21 protein within iLN ipsilateral and contralateral to the side of Td pre-conditioning from $n = 2$ mice with $n = 2$ technical replicates performed per iLN. Representative of three experiments. **c**, Increased lymph node CCL21 in *Ccl3*$^{-/-}$ hosts after CCL3 reconstitution and induction of Td recall response (all two group comparisons). CCL21 levels in bilateral iLNs of *Ccl3*$^{-/-}$ hosts after induction of Td recall response and CCL3 administration. Mixed model accounting for within-mouse correlation of measurements, *F*-test, $P < 0.001$; pairwise comparisons, WT Td plus Td i.d. ($n = 4$ iLNs) versus *Ccl3*$^{-/-}$ Td plus Td i.d. ($n = 3$ iLNs), $P = 0.045$; *Ccl3*$^{-/-}$ Td plus Td i.d. and CCL3 i.v. ($n = 4$ iLNs) versus *Ccl3*$^{-/-}$ Td plus Td i.d. and versus *Ccl3*$^{-/-}$ plus CCL3 i.v. ($n = 4$ iLNs), $P = 0.0066$ and $P = 0.026$, respectively. Scatter plot shows averaged values with $n = 2$ technical replicates performed per lymph node sampled. In **a** and **c**, mean ± s.e.m.

©2015 Macmillan Publishers Limited. All rights reserved

Extended Data Table 1 | Clinical trial patient characteristics

Patient	Sex	Age	Biopsy location	Race	KPS	WHO score	MMSE	IDH1	MGMT	*MGMT* promoter methylation	Vaccine site pre-conditioning	PFS (randomization)	OS (randomization)	PFS (diagnosis)	OS (diagnosis)	EORTC predicted median OS	EORTC O-E	RPA class	RPA O-E
1	F	46	R. frontal	W	100	0	29	-	N/A	N/A	Td	8.8	19.2	15.4	25.7	26.8*	-1.1	III	7.8
2	F	32	R. frontal	W	100	0	29	+	-	-	DC	21.7	35.2	27.8	41.3	13.0 ¶	28.3 ¶	III	23.4
3	M	62	R. temporal	W	90	1	29	-	-	-	DC	4.9	10.9	11.2	17.3	9.8	7.5	IV	6.2
4	M	71	L. frontoparietal	W	90	1	30	-	-	+	Td	41.4	41.4	47.3†	47.3‡	16.4	30.9	IV	36.2
5	M	43	L. temporal	W	90	1	28	-	-	+	DC	2.5	12.2	10.0	19.7	16.4	3.3	III	1.8
6	F	59	R. temporal	W	80	1	30	-	-	-	Td	39.5	39.5	45.0†	45.0‡	9.8	35.2	IV	33.9
7	M	75	R. temporal	B	90	1	26	-	+	+	Td	9.5	14.7	15.4	20.6	11.8	8.8	IV	9.5
8	F	58	L. parietal	H	90	1	22	-	+	N/A	DC	2.5	13.4	9.1	20.0	13.1*	6.9	IV	8.9
9	F	30	R. temporal	W	90	1	29	N/A	+	N/A	Td	36.6	36.6	44.1†	44.1‡	21.3*	22.8	III	26.2
10	F	66	L. frontoparietal	W	80	1	24	-	+	-	DC	3.9	9.5	10.4	16.0	6.9	9.1	IV	4.9
11	F	28	L. frontotemporal	W	100	0	28	-	-	-	DC	6.1	7.4	12.5	13.8	13.0	0.8	III	-4.1
12	M	59	R. posteroparietal	W	90	1	29	§	§	§	DC	§	§	5.1	19.0	18.1*	0.9	IV	7.9
13	M	71	L. posterotemporal	W	90	1	21	-	+	+	Td	12.7	15.2	18.5	20.9	11.8	9.1	IV	9.8
Median DC		58.5			90	1	28					4.4	11.6	10.8	18.5	13.0 ¶	6.9 ¶	IV	6.2
Median Td		65			90	1	29					NE	NE	NE	NE	14.1	>16	IV	>18

Demographic and prognostics factors of newly diagnosed GBM patients with vaccine site pre-conditioning randomization strategy and corresponding progression-free and overall survival from the time of surgery and from randomization to pre-conditioning. Observed and predicted survival times are expressed in months. Median values are shown for Td and unpulsed DC cohorts. Predicted median overall survival for RPA class yielded 17.9 months for class III and 11.1 months for class IV based on recursive partition analysis[15]. Model 3 of the EORTC scoring system that incorporated *MGMT* promoter methylation status, MMSE score, and WHO performance status was used to generate predicted median survival rates.

* Model 2 of EORTC scoring system if methylation status unavailable.

† No progression.

‡ Alive.

§ Patient progressed before time of randomization for vaccine site pre-conditioning.

EORTC, European Organization for Research and Treatment of Cancer; L, left; IDH1, isocitrate dehydrogenase type1; KPS, Karnofsky performance status; MGMT, O^6-methylguanine-DNA methyltransferase; MMSE, mini-mental state examination; NA, tissue not available; NE, not estimable; O−E, observed − expected survival months; OS, overall survival; PFS, progression-free survival; R, right; RPA, recursive partitioning analysis; WHO, World Health Organization.

©2015 Macmillan Publishers Limited. All rights reserved